Integrated Traction/Charge/Air Compression Supply using 3-Phase Split-windings Motor for Electric Vehicle

W. Lhomme, *Member, IEEE*, P. Delarue, T. J. Dos Santos Moraes,
N. K. Nguyen, *Member, IEEE*, É. Semail, *Member, IEEE*, K. Chen and B. Silvestre

***Abstract* — High cost, no-ideal driving range and charge time limit electric vehicle market share. Facing these challenges, an integrated motor drive/battery charger system has been proposed by Valeo. A further advancement, based on this system, is present in this paper; for the first time, the integration of traction, charging and air-compressor supply modes is proposed and tested by real-time experimentation. This integrated system is expected to increase the vehicle component compactness and power, therefore potentially reduce the cost and battery charging time. An overall and unique control scheme is detailed to achieve the three main operating modes: traction, charging and air-compressor supply modes. The real-time experimentation results show the system feasibility.**

***Index Terms*—Battery charger, Multiphase drive, Air-compressor, Automotive, Electric vehicle**

NOMENCLATURE

Variables		Subscripts	
C	Capacitance [F]	bat	Battery
e	Back EMF [V]	bus	DC bus
i	Electric current [A]	cr	Compressor
L	Inductance [H]	conv	Converter
M	Mutual [H]	dq	dq frame
r	Resistance [Ω]	g	Grid
s	Switching function [-]	h	Mid-points of the H-bridge
v	AC single phase voltage [V]	m	Motor
V	DC voltage [V]	odq	odq frame
u	AC phase-to-phase voltage [V]	p	Mid-points of the windings
T	Torque [Nm]	s	Switch element
α	Duty cycle [-]	tract	Traction subsystem
Φ	Magnetic flux [Wb]		
Ω	Rotational speed [rad/s]		

I. INTRODUCTION

Increasing pure electric driving range, decreasing the battery charge time and reducing vehicle costs are the three main challenges that automotive industry has to face for developing Electric Vehicle (EV). To meet the challenges, the key components are battery chargers, electrical machines and their power electronics. In most of the cases, the charger is installed in the vehicle, allowing the battery to be recharged anywhere a power outlet is available. However, in order to restrict the on-board charger size and weight, its power is limited. To turn vehicle components more compacted with higher power, many different integrated motor drive / battery charger solutions have been studied [1]-[17].

These integrated motor drive / battery charger solutions can be classified by single-phase or 3-phase AC supply [1]-[3]. The integrated charger using single-phase AC supply is, however, generally limited to low power charge ability. For integrated charger using 3-phase AC supply, several solutions have been proposed. In [4] Cocconi has presented an integrated motor drive / battery charger based induction or brushless DC motor with a set of relays. In [5] the authors have proposed an integrated motor drive / battery charger based on a wound-rotor induction motor. Recently a split-stator winding IPMSM has been proposed for an isolated high-power integrated charger [6]. Nevertheless, all of the above reference solutions generate motor torque during the charging and need a set of relays to reconfigure the motor between the traction and the charging modes. For safety reasons the generation of torque needs the use of a clutch or a mechanical rotor lock. To avoid rotating field into the motor a multiphase machine has to be used [7]. Subotic et al. have proposed to connect the 3-phase AC supply to the neutral points of isolated 3-phase windings of an N-leg inverter. N is a multiple of 3 with at least 9 phases [8]. Some solutions based on 6-phase drives have also been proposed. In [9] two topologies of an isolated charger are proposed according to the stator windings, asymmetrical or symmetrical, of the 6-phase induction machine. The case with an asymmetric 6-phase requires a transformer with dual secondary that creates a 6-phase voltage supply. The machine is supposed to have a sinusoidal magnetomotive force (MMF) and the torque is only created by the 1st harmonic of currents: a sinusoidal rotating field in the αβ frame. In this work a phase transposition between the output of grid, with or without the transformer, and the 6-phase machine is required to impose a zero torque during the charging/vehicle to grid modes and a hardware reconfiguration is required to

W. Lhomme, P. Delarue, T. J. Dos Santos Moraes, N. K. Nguyen and E. Semail are with the Univ. Lille, Centrale Lille, Arts et Métiers Paris Tech, HEI, EA 2697 L2EP - Laboratoire d'Electrotechnique et d'Electronique de Puissance F-59000 Lille, France (e-mail: walter.lhomme@univ-lille1.fr; philippe.delarue@univ-lille1.fr; tiago.dossantosmoraes@ensam.eu; eric.semail@ensam.eu; ngacky.nguyen@ensam.eu).

K. Chen and B. Silvestre are with Valeo Siemens eAutomotive France SAS F-95000 Cergy, France (e-mail: keyu.chen.jv@valeo-siemens.com, benedicte.silvestre.jv@valeo-siemens.com).

switch between the traction and the charging mode. In [10], a topology for 3-phase charging and 6-phase traction modes has been proposed for a 6-phase symmetrical machine by using only a 9 switch inverter, instead of 12. During the charging mode, controlling the middle switch of the 9-switch inverter and an additional hardware reconfiguration, composed of 9 switches, leads the 6-phase symmetrical machine become a classical 3-phase machine.

According to Levi [7], the most developed integrated motor drive / battery charger is based on the concept of [11]-[13] with associated optimized controls using numerous degrees of freedom of the structure [14]-[15]. [11] and [12] are the first patents of this concept to present the invention of the automotive supplier Valeo, which describes an integrated 3-phase split-winding electrical machine and on-board battery charger system without static relays. In [13] De Sousa et al. presents, in terms of performances and efficiencies, the comparison of this integrated system with the classical solution using a 3-leg inverter with its 3-phase electrical machine and a battery charger. The concept uses a split-windings AC motor with just a 6-leg inverter instead of at least 9 in [8]. The middle point of each phase windings is connected to the 3-phase supply to achieve charging mode. This technology ensures that, during charging mode, the rotor of the electrical machine does not vibrate or rotate, because the winding configuration allows decoupling magnetically the rotor and the stator of the electrical machine. No motor reconfiguration and no supplementary static relays are necessary. It may be noted that the traction mode has already been studied in the flux-weakening region [15] and in degraded mode [16]. A space-vector pulse width modulation (SVPWM) of the 6-leg inverter has furthermore been proposed in [17].

In this paper, based on the concept of [11]-[13], a further advancement is proposed to not only combine in a unique system the traction and charging, but also to provide an auxiliary system supply in traction mode: the air-compressor supply of the air-conditioning. It has been demonstrated that several electrical machines could be connected in series with an appropriate connection using a single inverter, with which an independent control for each motor can be implemented [18]. The middle point of the split-windings of each phase can then be connected to another electrical machine, in this paper, an air compressor during the traction mode. All in all, the 6-leg inverter achieves the functions of propulsion, charging and air-conditioning. As the number of the inverter legs is reduced, the cost, volume and weight are potentially reduced.

The objective of this paper is to show the feasibility of this integrated system that combines the traction / charge / air-compression supply modes by experimental results. Prior to this paper, it is the first time to show the three modes experimental results of this innovative system. To deal with the complexity of the multi-phase system the Energetic Macroscopic Representation (EMR) will be used [19]-[21]. A unified control scheme is deduced from this EMR to achieve the three operation modes.

Section 2 presents the electrical architecture of the vehicle with the combined electrical drive / battery charger / air-compression supply. The modeling, the description and the overall control of the system are dealt with in section 3. Finally, experimental results with discussions are presented in section 4.

II. Electrical Architecture of the Integrated 3-Phase Split-windings Motor of the Vehicle

A. Studied system

The original concept in [11]-[13] uses a common power electronic converter to propel the vehicle or charge the battery at a standstill. A 6-leg inverter supplies a 3-phase open-end winding motor with an accessible central point per phase. Six of the connection points (a, a', b, b', c and c' in Fig. 1) are connected to the inverter legs, in order to supply the three phases. The other three connection points (1, 2 and 3) are connected to the 3-phase AC system.

During charge mode, the motor windings compose the charger system. As the charger windings' cost and weight are directly related to its charging power, this sharing of the motor windings results in a considerable gain of weight and cost in comparison to other proposed structures, in which the charger has its own windings. Moreover, the windings of the system present in this paper are sized to ensure the traction function of the electric motor, whose power is equivalent of a standard high power charger: 22 kW. As a conclusion, no supplementary cost or volume is needed in order to ensure its traction and charging functions. A buck-boost converter is set between the battery and the 6-leg inverter. A constant DC bus voltage is then ensured. The constraint of the battery charger is then satisfied with a high value on the voltage whatever the depth of discharge level of the battery. Compared to other charging systems, the concept proposed is an economic and compact on-board solution, compatible with any type of grids, whatever the way of energy flow: battery charger mode or vehicle-to-grid mode.

The 6-leg inverter is used either for the traction mode or for the charging mode, never at the same time. The 6-leg inverter can be seen as 3 independent 2-leg inverter. Each 2-leg inverter is used to supply one of the 3 phases of the electrical machine. A classical 3-leg inverter has 8 ($=2^3$) different states. A 6-leg inverter presents then 64 ($=2^6$) different states, which leads to more degrees of freedom to be used to optimize the modulation or to control the zero sequence current inside the machine. More information regarding fundamental principles of a 6-leg inverter can be found in [22]. Levi et al. [18] has nevertheless demonstrated that it was possible to decouple the control of two series-connected multi-phase machines, even though they are supplied by the same inverter. During the propulsion mode the mid-points of the windings can then be used to supply another electrical machine. In this paper, the electrical machine will be the air compressor of the air conditioning. A switch element is required to switch between charging and air compression mode. Both used electrical machines are considered as Permanent Magnet Synchronous Machine (PMSM).

B. Operating modes

Depending on the switching element state, different operating modes can be done. Table 1 summarizes all the operating modes for the currents of the mid-point of the winding 1 and the phase-to-phase voltages. In traction mode, the 3-phase open-end winding PMSM is used by controlling its currents. Since a source or a load can be connected to the mid-points of the 3-phase, the machine currents $\underline{i_m}$ of the traction mode are not directly given. In traction mode we have chosen, imposed by the control, to set the machine current $\underline{i_m}$ as half of the difference of

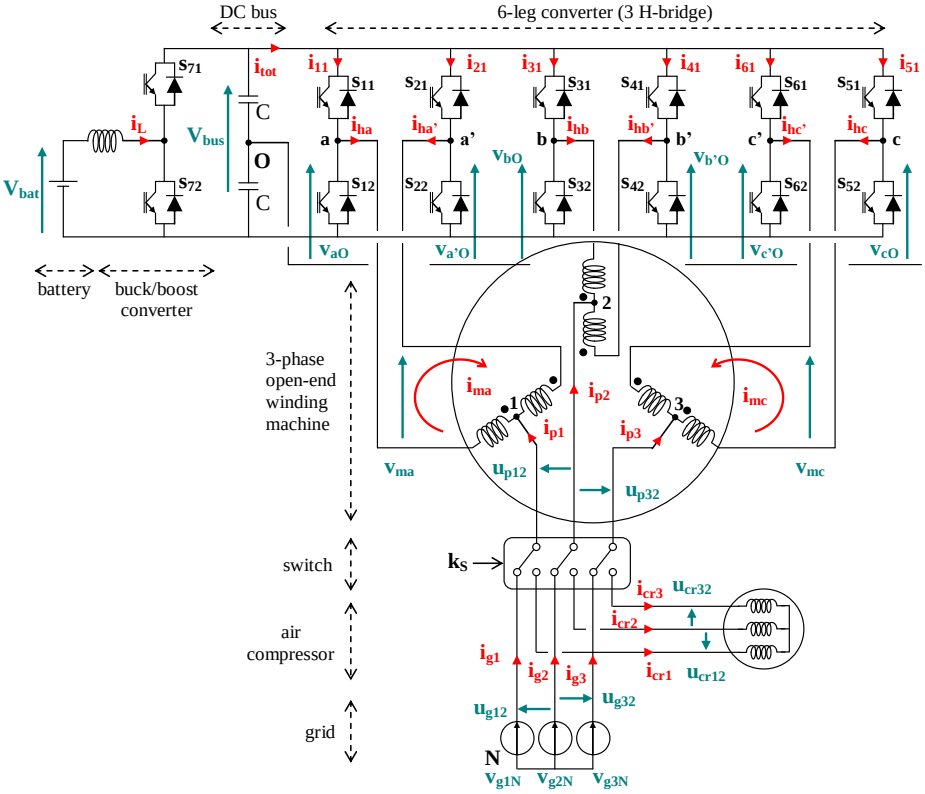

Fig. 1. The studied 3-phase open-end winding system

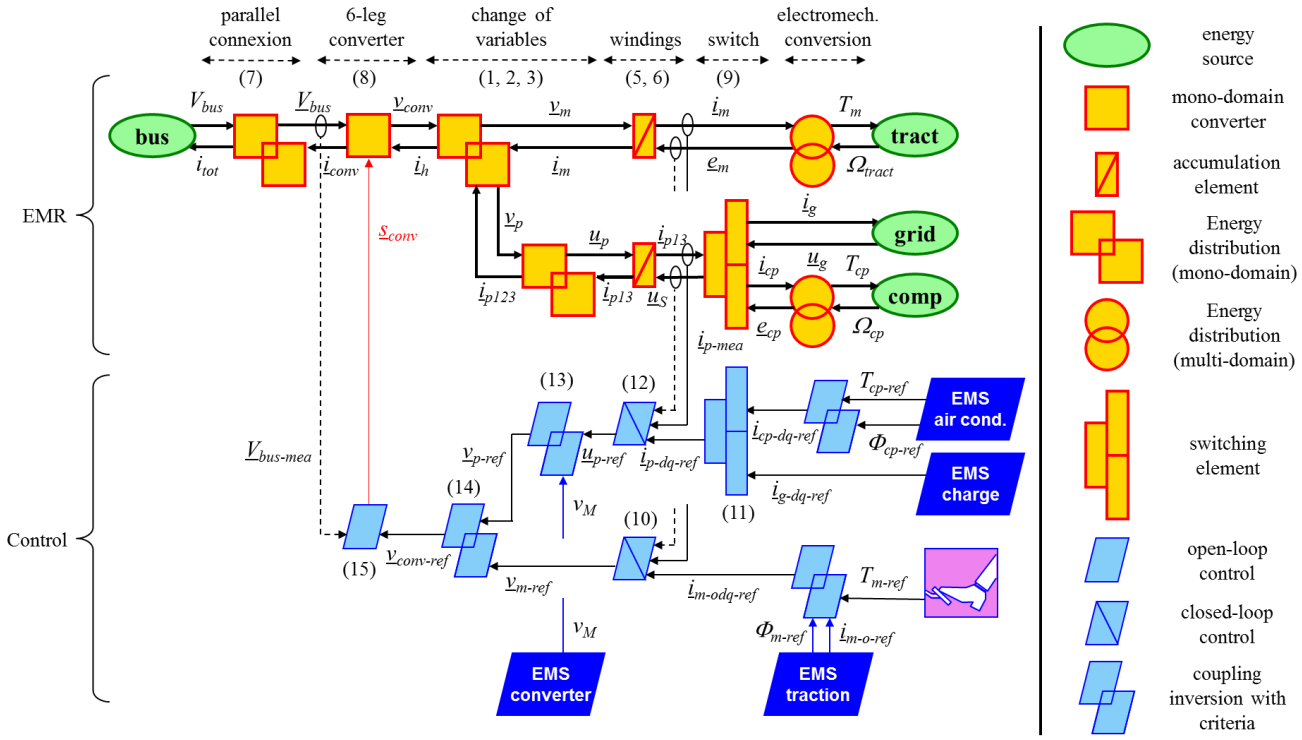

Fig. 2. Energetic Macroscopic Representation and its control of the studied 3-phase open-end winding machine

leg currents i_{hX} and $i_{hX'}$ with $X \in [a, b, c]$. The single-phase voltage of the machine $\underline{v}_m$ corresponds to the voltage applied on the phases, i.e. two half-windings:

$$\begin{cases} \underline{i}_m = \frac{1}{2} T_1 \underline{i}_h \\ \underline{v}_m = T_1 \underline{v}_{conv} \end{cases} \text{ with } T_1 = \begin{bmatrix} -1 & 1 & 0 & 0 & 0 & 0 \\ 0 & 0 & -1 & 1 & 0 & 0 \\ 0 & 0 & 0 & 0 & -1 & 1 \end{bmatrix}$$
$$\begin{cases} \underline{i}_h = [i_{ha} \quad i_{ha'} \quad i_{hb} \quad i_{hb'} \quad i_{hc} \quad i_{hc'}]^t \\ \underline{v}_{conv} = [v_{aO} \quad v_{a'O} \quad v_{bO} \quad v_{b'O} \quad v_{cO} \quad v_{c'O}]^t \end{cases} \quad (1)$$
$$\text{and} \begin{cases} \underline{i}_m = [i_{ma} \quad i_{mb} \quad i_{mc}]^t \\ \underline{v}_m = [v_{ma} \quad v_{mb} \quad v_{mc}]^t \end{cases}$$

When the system is in traction mode, the machine's phase currents i_{mX} are equal to the currents of the leg: $i_{mX} = i_{hX} = -i_{hX'}$ with $X \in [a, b, c]$.

III. Modeling and Control: Systemic Approach

A. Modeling

Change of variables – The aim of the change of variables is to decompose the 3-phase open-end winding machine in two fictitious machines (Fig. 3). The first fictitious machine is a 3-phase 4-wire machine used to create the torque T_m in the traction mode. The second fictitious machine does not create torque (T_1=0). It is then equivalent to three inductors.

The first change of variables (1) leads to calculate, from the six actual currents $\underline{i}_h$ and voltages $\underline{v}_{conv}$, the three independent fictitious currents $\underline{i}_m$ and voltages $\underline{v}_m$ of the fictitious 3-phase 4-wire machine. The second change of variables (2) allows writing the relationships of the mid-points of the windings:

$$\begin{cases} \underline{i}_{p123} = -T_2 \underline{i}_h \\ \underline{v}_p = \frac{1}{2} T_2 \underline{v}_{conv} \end{cases} \text{ with } T_2 = \begin{bmatrix} 1 & 1 & 0 & 0 & 0 & 0 \\ 0 & 0 & 1 & 1 & 0 & 0 \\ 0 & 0 & 0 & 0 & 1 & 1 \end{bmatrix} \quad (2)$$
$$\text{and} \begin{cases} \underline{i}_{p123} = [i_{p1} \quad i_{p2} \quad i_{p3}]^t \\ \underline{v}_p = [v_{p1} \quad v_{p2} \quad v_{p3}]^t \end{cases}$$

TABLE I. Currents and Voltages According to the Operating Modes

Mode	Currents	Voltages
Charging	$i_{cr1} = 0$ $i_{ma} = 0$ $i_{g1} = i_{p1} = -2i_{ha} = -2i_{ha'}$	$\begin{cases} u_{g12} = u_{p12} \\ u_{g32} = u_{p32} \end{cases}$ $\begin{cases} u_{cr12} = 0 \\ u_{cr32} = 0 \end{cases}$
Traction	$i_{cr1} = i_{p1} = 0$ $i_{ma} = i_{ha'} = -i_{ha}$ $i_{g1} = 0$	$\begin{cases} u_{g12} = 0 \\ u_{g32} = 0 \end{cases}$ $\begin{cases} u_{cr12} = u_{p12} \\ u_{cr32} = u_{p32} \end{cases}$
Air Compression	$i_{cr1} = i_{p1} = -2i_{ha} = -2i_{ha'}$ $i_{ma} = 0$ $i_{g1} = 0$	$\begin{cases} u_{g12} = 0 \\ u_{g32} = 0 \end{cases}$ $\begin{cases} u_{cr12} = u_{p12} \\ u_{cr32} = u_{p32} \end{cases}$
Traction + Air Compression	$i_{cr1} = i_{p1} = -i_{ha} - i_{ha'}$ $i_{ma} = (i_{ha'} - i_{ha})/2$ $i_{g1} = 0$	$\begin{cases} u_{g12} = 0 \\ u_{g32} = 0 \end{cases}$ $\begin{cases} u_{cr12} = u_{p12} \\ u_{cr32} = u_{p32} \end{cases}$

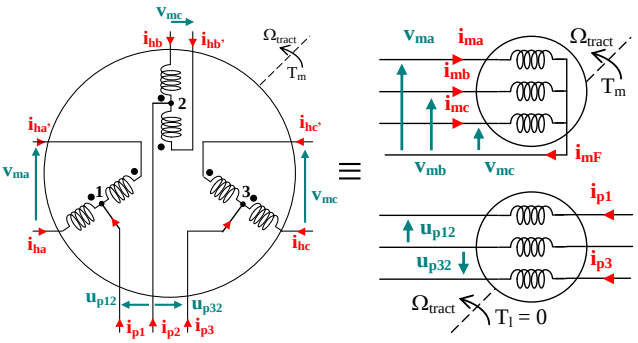

Fig. 3. Equivalence between the 3-phase open-end winding machine and two 3-phase machines

Due to the architecture, the open-end winding electrical machine is not electrically coupled. The three currents i_{ma}, i_{mb} and i_{mc} then have to be controlled to produce the torque T_m. Since the mid-point connection has three wires, only two control currents are sufficient for control purpose: i_{p1} and i_{p3}. The relationship (2) then has to be rewritten with these currents and the phase-to-phase voltages $\underline{u}_p$:

$$\begin{cases} \underline{i}_{p123} = T_3^t \underline{i}_{p13} \\ \underline{u}_p = T_3 \underline{v}_p \end{cases} \text{ with } T_3 = \begin{bmatrix} 1 & -1 & 0 \\ 0 & -1 & 1 \end{bmatrix}$$
$$\text{and} \begin{cases} \underline{i}_{p13} = [i_{p1} \quad i_{p3}]^t \\ \underline{u}_p = [u_{p12} \quad u_{p32}]^t \end{cases} \quad (3)$$

Electrical windings – The design of the electrical machine leads to a strong magnetic coupling between each of the half-phases. Considering six identical windings and neglecting saliency effects, the inductor matrix L_{EM} of the electrical machine can be written such as:

$$L_{EM} = \begin{bmatrix} L + l_l & -L & M & -M & M & -M \\ -L & L + l_l & -M & M & -M & M \\ M & -M & L + l_l & -L & M & -M \\ -M & M & -L & L + l_l & -M & M \\ M & -M & M & -M & L + l_l & -L \\ -M & M & -M & M & -L & L + l_l \end{bmatrix} \quad (4)$$

In relation (4), L is the half-winding's inductance, l_l represents the leakage inductance and the mutual inductance between half-windings is noted M.

The change of variables (1) and (2) leads to write (5) and (6) for the two fictitious machines:

$$\underline{v}_m - \underline{e}_m = \frac{d}{dt}[L_m \underline{i}_m] + r_m \underline{i}_m$$
$$\text{with } L_m = 4 \begin{bmatrix} L + l_l/2 & M & M \\ M & L + l_l/2 & M \\ M & M & L + l_l/2 \end{bmatrix} \quad (5)$$
$$\text{and } r_m = 2\, r_s \begin{bmatrix} 1 & 0 & 0 \\ 0 & 1 & 0 \\ 0 & 0 & 1 \end{bmatrix}$$

$$\underline{u}_S - \underline{u}_p = \frac{d}{dt}[L_p \underline{i}_{p13}] + r_p \underline{i}_{p13}$$
$$\text{with } L_p = \frac{l_l}{2} \begin{bmatrix} 2 & 1 \\ 1 & 2 \end{bmatrix} \text{ and } r_p = \frac{r_s}{2} \begin{bmatrix} 2 & 1 \\ 1 & 2 \end{bmatrix} \quad (6)$$

Relations (5) and (6) form a five-order system of differential equations. Nevertheless the equations between both fictitious machines are totally decoupled.

Energy sources – The paper is focused on the PMSM control of the different operating modes: traction, charging and air compression. An electrical source connected to the DC bus is considered to represent the battery and the associated chopper. An equivalent mechanical load represents the traction subsystem. The torque T_m of the electrical machine acts on this load, the reaction is the speed Ω_{tract}. The 6-leg converter is supplied by the DC bus with a voltage V_{bus}, the reaction is the current i_{tot}. The system is supplied by the grid voltages $\underline{u_g}$ and reacts by circulating currents $\underline{i_g}$.

6-leg power converter – The switch orders are mathematically represented by switching functions s_{ij}. These functions are equal to 0 when switches are open and equal to 1 when switches are closed. The DC bus V_{bus} and switching functions s_{ij} lead to determine the rectifier voltages $\underline{v_{conv}}$. As well as, converter current i_h and and switching functions s_{ij} leads to determine the DC bus current i_{conv} and then i_{tot}.

$$i_{tot} = I\ \underline{i_{conv}} \text{ with I the unitary matrix of size 1 X 6}$$
$$\text{and } \underline{i_{conv}} = [i_{11} \quad i_{21} \quad i_{31} \quad i_{41} \quad i_{51} \quad i_{61}]^t \tag{7}$$

$$\begin{cases} \underline{v_{conv}} = \left(\underline{s_{conv}} - \frac{1}{2}\right) V_{bus} \\ \underline{i_{conv}} = \underline{s_{conv}} \underline{i_h} \end{cases}$$
$$\text{with } \underline{s_{conv}} = [s_{11} \quad s_{21} \quad s_{31} \quad s_{41} \quad s_{51} \quad s_{61}]^t \tag{8}$$
where $s_{ij} \in \{0;1\}$ with $i \in \{1;2;3;4;5;6\}$ the number of the legs
and $j \in \{1;2\}$ the number of the switch in the leg

Switch element – The switch element commutes through the grid currents or the air compressor currents based on the value of the switch input k_S:

$$\begin{cases} \underline{u_S} = k_S \underline{u_g} + (1 - k_S) \underline{e_{cp}} \\ \underline{i_{p13}} = k_S \underline{i_g} + (1 - k_S) \underline{i_{cp}} \end{cases} \text{ with } k_S \in \{0;1\} \tag{9}$$

Electromechanical conversion – The electrical machine leads to the torque T_m and the back EMF $\underline{e_m}$. The currents of the machine are noted $\underline{i_m}$ and the rotation speed Ω_{tract}. The modeling of the machine can be found in [15].

B. Energetic Macroscopic Representation

EMR is a functional description of energetic systems for control purpose [19]-[21]. The system is split into elementary subsystems in interaction. According to the action and reaction principle all subsystems are interconnected. The instantaneous power flow between two subsystems is the product of the action and reaction variables. In EMR, only the integral causality must be used: outputs are integral functions of inputs. This property is described with accumulation elements. Other elements are defined using equations without time dependence. The EMR of the studied architecture, without the air compressor, has been proposed in [23] (upper part in Fig. 2). For better clarity all variables are defined as vectors. The DC bus and the grid are considered as electrical sources (green oval pictograms). The air compression and the traction subsystems are considered as mechanical sources. The inverter performs mono-domain conversions (orange square pictograms). The parallel connection couples each leg of the 6-leg inverter and the change of variables is represented by a mono-domain distribution element (overlapping squares). The inductors are accumulation elements (orange rectangle pictograms with diagonal line). The currents of the machine $\underline{i_m}$ and the mid-points of the windings $\underline{i_p}$ are the five state variables of the studied system.

C. Inversion-based control scheme

From inversion rules, EMR can deduce an inversion-based control scheme. Two kinds of levels are organized: local and global controls. The local control level controls the different subsystems. It is described by light blue parallelograms in Fig. 2. The global control level is the EMS, which stands for Energy Management Strategy. The EMS coordinates the local control to manage the whole system. It is described by dark blue parallelograms in Fig. 2. In this study, there are two main control objectives. The first objective is to impose the torque of the machine T_m through the currents $\underline{i_m}$. The second objective is to impose the currents of the grid $\underline{i_g}$ for the charging mode, or the torque of the air compressor T_{cp} for the air compressor mode, through the currents $\underline{i_p}$. Six tuning variables, the switching functions $\underline{s_{conv}}$, are managed to reach this aim. From the objectives to the switching functions, the local control can then be deduced by inverting the EMR. The accumulation elements is inverted with the crossed blue parallelograms, which correspond to closed-loop controls. The conversion elements with the blue parallelograms, which correspond to an open-loop control. The energetic coupling is inverted with the overlapped blue parallelograms.

The control of the three currents of the electrical machine $\underline{i_m}$ allows controlling the torque T_m and the magnetic flux Φ_m (EMS traction). To simplify the calculations of the control direct-quadrature-zero transformation is used. Comparing to wye-connected structures, this topology has one more degree of freedom (DoF) consisting in the possibility to have the zero sequence current $i_{m\text{-}o\text{-}ref}$. Based on this DoF, different studies have been proposed. Indeed, in [15] the homopolar current is used to extend the range of speed with a higher torque for a 3-phase PMSM during flux weakening operation. In case of open-phase fault, having the homopolar component reduces torque ripples [24]-[26]. In [27], using $i_{m\text{-}o\text{-}ref}$ leads to minimum copper losses for a given torque in case where the back-EMF contains harmonics k*n (n: the number of phases, k=1, 2,…). The work presented in [27] is available not only for 3-phase drives but also for multiphase drives.

Currents in rotating frame are controlled by PI controllers $\underline{C_{m-odq}}$ since their references are constant. The machine voltages are thus determined as shown in (10).

$$\begin{gathered} \underline{v_{m-odq-ref}} = \underline{C_{m-odq}}\left(\underline{i_{m-odq-ref}} - \underline{i_{m-odq-est}}\right) + \underline{e_{m-odq-est}} \\ \underline{v_{m-ref}} = P(\theta)^{-1} \underline{v_{m-odq-ref}} \\ \underline{i_{m-odq-est}} = P(\theta) \underline{i_{m-mea}} \\ P(\theta) = \sqrt{\frac{2}{3}} \begin{bmatrix} \cos(\theta) & \cos\left(\theta - \frac{2\pi}{3}\right) & \cos\left(\theta + \frac{2\pi}{3}\right) \\ -\sin(\theta) & -\sin\left(\theta - \frac{2\pi}{3}\right) & -\sin\left(\theta + \frac{2\pi}{3}\right) \\ \frac{\sqrt{2}}{2} & \frac{\sqrt{2}}{2} & \frac{\sqrt{2}}{2} \end{bmatrix} \end{gathered} \tag{10}$$

The control of the mid-points currents $\underline{i_{p13}}$ depends of the chosen operating mode through the input switch k_S.

$$\underline{i_{p-dq-ref}} = k_S \underline{i_{g-dq-ref}} + (1 - k_S) \underline{i_{cp-dq-ref}} \tag{11}$$

In the charging mode, when $k_S = 1$, the objective of the control is to manage the charge of the battery from the grid. Two grid currents $\underline{i}_{g\text{-}dq\text{-}ref}$ leads to control active and reactive power on the grid. A classical Power Factor Correction is used in this purpose inside of the "EMS charge". The grid current references are calculated, according to the power of charging, from the grid voltages. Because PI controllers are used for tracking the currents, it should be better to have constant references of current by using a Phase-Locked Loop (PLL) for frame rotation. The grid currents are only used in case of charging. The voltage references are thus determined as given in (12).

$$\begin{aligned} \underline{u}_{p-dq-ref} &= -\underline{C}_{p-dq}\left(\underline{i}_{p-dq-ref} - \underline{i}_{p-dq-est}\right) + \underline{u}_{S-est} \\ \underline{u}_{p-ref} &= P(\theta)^{-1}\underline{u}_{p-dq-ref} \end{aligned} \quad (12)$$

The second coupling element of the EMR, "change of variables" in Fig. 2, deduces the two phase-to-phase voltages of the mid-points of the windings $\underline{u}_p$ from the three single phase voltages of the mid-points $\underline{v}_p$. This change of variable that is non-bijective, leads to the homopolar voltage v_M:

$$\begin{aligned} &\underline{v}_{p-ref} = \underline{v}_{K-ref} + v_M \\ &\text{with } \underline{v}_{K-ref} = T_4\underline{u}_{p-ref} \text{ where } T_4 = \\ &\frac{1}{3}\begin{bmatrix} 2 & -1 \\ -1 & -1 \\ -1 & 2 \end{bmatrix} \\ &\qquad v_{1K-ref} + v_{2K-ref} + v_{3K-ref} = 0 \\ &\text{and } \underline{v}_{K-ref} = \\ &[v_{1K-ref} \quad v_{2K-ref} \quad v_{3K-ref}]^t \end{aligned} \quad (13)$$

$$\underline{v}_{conv-ref} = \begin{bmatrix} T_1 \\ \frac{1}{2}T_2 \end{bmatrix}^{-1} \begin{bmatrix} \underline{v}_{m-ref} \\ \underline{v}_{p-ref} \end{bmatrix} \quad (14)$$

The homopolar voltage v_M can be considered as a DoF to increase the modulation index of the converter using over-modulation techniques in case of wye-connection since there is no path for zero sequence of current. In this paper, choosing $v_M = 0$ is necessary to eliminate $i_{m\text{-}o\text{-}ref}$ because of the sinusoidal back-EMF.

The coupling inversion element leads then to the six converter reference voltages $\underline{v}_{conv\text{-}ref}$ from the two grid reference voltages $\underline{u}_{l\text{-}ref}$, the three motor reference voltages $\underline{v}_{m\text{-}ref}$ and the homopolar voltage $\underline{u}_{h\text{-}ref}$. The duty cycle of the switching function $\underline{\alpha}_{conv\text{-}ref}$ are obtained by an inversion of (8):

$$\underline{\alpha}_{conv-ref} = \frac{\underline{v}_{conv-ref}}{V_{bus-meas}} + \frac{1}{2} \quad (15)$$

A Pulse Width Modulation (PWM) is then classically used to define the switching function references $\underline{s}_{conv\text{-}ref}$ from this duty cycle.

The proposed control of the entire system in Fig. 2 can seem complicated but, in fact, it is no more complex than a classical control of a 3-phase electrical machine for the traction mode and a classical control of a 3-phase PWM converter for the battery charger or for supplying the compressor. Current controllers in rotating frames have been used in the control scheme. The current references are obtained from the torque in traction mode and from the required power for air compressor / charging. Regular PI controllers are used since all currents in rotating frames are constant. The only differences are inversions of coupling relations implemented by relations (11) and (14) that are not so complicated to implement and which do not consume lots of execution time.

IV. Results and Discussion

To test the system, the studied structure is presented in Fig. 4. The grid and the air compressor are represented by an electrical drive, which will work as a generator in charging mode and as motor in compression mode. A test bench built for this experiment is reported in Fig. 5. It is composed of:

- two isolated DC-sources;
- an industrial drive to simulate the load for both emulators;
- a current measurement box and a dSPACE MicroLabBox to carry out the proposed control. The MicroLabBox is an equipment of dSPACE with a high calculation capacity up to 2GHz for real-time processor. During the tests, the fixed-step calculation has been set up at 100 µs in Simulink control scheme. The switching frequency has been fixed at 10 kHz;
- a mechanical load of 10 kW to emulate the grid and the air compressor;
- a 3-phase open-end winding PMSM of 15 kW with its 6-leg inverter connected mechanically to a load drive to emulate the traction subsystem, and connected electrically at the mid-points of the windings to a 3-phase PMSM. The 3-phase open-end winding PMSM has 12 windings and 8 poles with a buried magnets rotor. The Back-EMF is almost sinusoidal and the main parameters of the machine is (see equation (5)): $r_s = 238\ m\Omega$; $L + l_l/2 = 1.44\ mH$; $M = -678\ \mu H$.

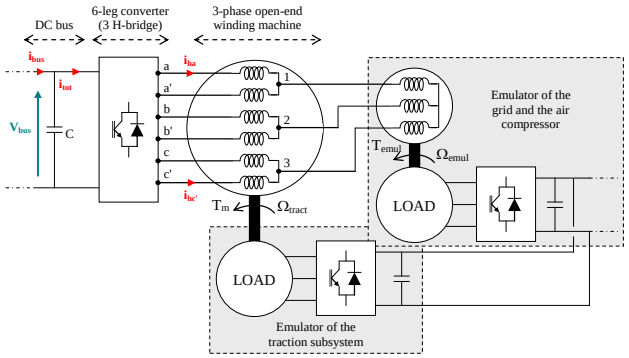

Fig. 4. Experimental set-up scheme

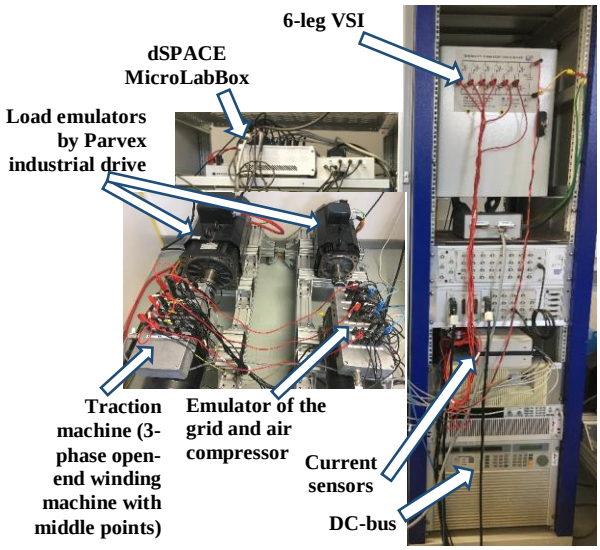

Fig. 5. Test bench

A profile test has been carried out to examine the different operating modes (Table II). Fig. 6 reports the experimental results for example functioning cycle having three modes: charging (I), traction (II) and traction plus compression (III).

The speeds of both machines and the DC bus current are shown in Fig. 6a. The emulated grid currents and references of voltage are reported in Fig. 6b and Fig. 6e. The currents and voltage references of the 3-phase open-end machine are given in Fig. 6c and Fig. 6d.

During the charging mode, the torque T_m is controlled to zero, then the speed is also zero. The speed of the machine emulating the 3-phase grid is setting to 80 rad/s. The measured DC bus current i_{bus}, similar to the battery power, is negative showing that the battery is in charging mode; at this time the grid currents are sinusoidal. It can be seen that the relation given in Table I for charging mode is verified by observing the currents of the two machines. Indeed, for example, $i_{p1} = -2\, i_{ha} = -2\, i_{ha'}$ leads to the current $i_{ma} = 0$ and as a consequence, the torque T_m generated by the 3-phase open-end winding machine is equal to zero. The emulated grid voltages are however not perfectly sinusoidal (Fig. 6e left side) due to some harmonics of the back-EMF, mainly the 3rd one, existing in the 3-phase machine used for the emulation of the grid.

In traction mode (mode II), only the 3-phase open-end winding machine is controlled to track a reference speed, which is fixed at 50 rad/s. The DC bus current i_{bus} becomes positive in this mode (Fig. 6a). During the traction mode, the currents of the 3-phase open-end winding machine are balanced with a phase-shifted of 60 degrees. This means that $i_{ha} = -i_{ha'}$, $i_{hb} = -i_{hb'}$ and $i_{hc} = -i_{hc'}$ (Fig. 6c right side) and $i_{p1} = i_{p2} = i_{p3} = 0$ (Fig. 6b middle). The voltage references of the traction machine are given in Fig. 6. These voltages are determined by PI current controllers and considered as voltages of a symmetric 6-phase wye-connected machine.

In mode III, i.e when the air compressor is started at 5.56s during the traction mode, the currents crossing the 3-phase open-end machine are unbalanced due to the different speeds of both machines. The change of torque for the 3-phase PMSM emulating air compressor at 7.05 s can be seen with the value of the currents in Fig. 6b right side.

The above presented results confirm the validity of the proposed structure for automotive applications by offering three operating modes by control strategies. The results given in Fig. 6 confirm that all the calculation are finished in time into the MicroLabBox. To prove the feasibility of the proposed control scheme the grid and the air compressor have been emulated with a versatile scaled-down prototype using a same PMSM. To better emulate the characteristics of the grid, a large PMSM with a small synchronous reactance and low total harmonic distortion (THD) would be preferable. Nevertheless the balanced 3-phase currents during the charging mode prove the feasibility even if the voltage of the grid contains harmonics. For the future, the real grid and a PMSM with a smaller power rating of the air compressor would be necessary to check the effectiveness of the control in real-world application scenarios.

TABLE II. PROFILE TEST

Mode	*3-phase open-end winding machine*	*3-phase machine (grid/air compressor)*
Charging (*Mode I*)	Speed and torque null	Generator with constant speed and torque
Traction (*Mode II*)	Acceleration then constant speed	Speed and torque null
Traction + Compression (*Mode III*)	Speed constant then deceleration	Motor with constant speed and 2 steps of torque

V. CONCLUSION

Using a split-windings AC motor, an integrated motor drive/battery charger/air-compressor supply system has been introduced and shown its feasibility by real-time experimentation. This paper describes the unique control, in a same structure, to achieve the three operating modes: charging, traction and air-compressor supply. The integrated system proposed in this paper is expected to increase the vehicle component compactness and power, therefore potentially reduces the cost and battery charging time. In future prospects, more potentialities of this integrated system will be studied, discussed and tested.

REFERENCES

[1] S. Haghbin, S. Lundmark, M. Alakula, and O. Carlson, "Grid-connected integrated battery chargers in vehicle applications: review and new solution", IEEE trans. on Industrial Electronics, vol. 60, no. 2, pp. 459-473, February 2013.

[2] N. Sakr, D. Sadarnac and A. Gascher, "A review of on-board integrated chargers for electric vehicles", 2014 16th European Conference on Power Electronics and Applications, Lappeenranta (Finland), pp. 1-10, August 2014.

[3] A. Khaligh, S. Dusmez, "Comprehensive topological analysis of conductive and inductive charging solutions for plug-in electric vehicles", IEEE trans. on Vehicular Technology, vol. 61, pp. 3475-3489, 2012

[4] A. G. Cocconi, "Combined motor drive and battery recharge system", US Patent no. 5,341,075, 23 August 1994

[5] F. Lacressonniere and B. Cassoret, "Converter used as a battery charger and a motor speed controller in an industrial truck", Proc. Eur. Conf. Power Electron. Appl., 2005, pp. 7.

[6] S. Haghbin, S. Lundmark, M. Alakula, and O. Carlson, "An isolated high-power integrated charger in electrified-vehicle applications", IEEE trans. Vehicular Technology, vol. 60, no. 9, pp. 4115–4126, November 2011.

[7] E. Levi, "Advances in converter control and innovative exploitation of additional degrees of freedom for multiphase machines", IEEE trans. on Industrial Electronics, vol. 63, no. 1, pp. 433-448, January 2016.

[8] I. Subotic, N. Bodo, E. Levi, and M. Jones, "On-board integrated battery charger for EVs using an asymmetrical nine-phase machine", IEEE trans. on Industrial Electronics, vol. 62, no. 5, pp. 3285–3295, May 2015.

[9] I. Subotic, N. Bodo, E. Levi, M. Jones, and V. Levi, "Isolated Chargers for EVs Incorporating Six-Phase Machines," IEEE Transactions on Industrial Electronics, vol. 63, pp. 653-664, 2016.

[10] M. S. Diab, A. A. Elserougi, A. S. Abdel-Khalik, A. M. Massoud, and S. Ahmed, "A Nine-Switch-Converter-Based Integrated Motor Drive and Battery Charger System for EVs Using Symmetrical Six-Phase Machines," IEEE Transactions on Industrial Electronics, vol. 63, pp. 5326-5335, 2016.

[11] L. De-Sousa, B. Bouchez, "Combined electric device for powering and charging", International Patent WO 2010/057892 A1

[12] L. De-Sousa, B. Bouchez, "Method and electric combined device for powering and charging with compensation means", International Patent WO 2010/057893 A1

[13] L. De Sousa, B. Silvestre, and B. Bouchez, "A combined multiphase electric drive and fast battery charger for electric vehicles", Proc. of IEEE VPPC 2010, Lille, France, September 2010

[14] A Bruyere, X Kestelyn, E Semail, P Sandulescu, F Meinguet, "Rotary drive system, method for controlling an inverter and associated computer program", US Patent 9,276,507, 2016.

[15] P. Sandulescu, F. Meinguet, X. Kestelyn, E. Semail, A. Bruyère, "Control strategies for open-end winding drives operating in the flux-weakening region", IEEE trans. on Power Electronics, vol. 29, pp. 4829-4842, 2014.

[16] O. Béthoux, E. Labouré, G. Remy and E. Berthelot, "Real-time optimal control of a 3-phase PMSM in 2-phase degraded mode," in IEEE trans. on Vehicular Technology, vol. 66, no. 3, pp. 2044-2052, March 2017.

[17] A. Kolli, O. Béthoux, A. De Bernardinis, E. Labouré and G. Coquery, "Space-vector PWM control synthesis for an H-bridge drive in electric vehicles", IEEE trans. on Vehicular Technology, vol. 62, no. 6, pp. 2441-2452, July 2013

[18] E. Levi, M. Jones, and S. N. Vukosavic, "Even-phase multi-motor vector controlled drive with single inverter supply and series connection of stator windings", IEE Proceedings - Electric Power Applications, vol. 150, no. 5, p. 580, September 2003.

[19] A. Bouscayrol, J.P. Hautier, and B. Lemaire-Semail, "Graphic formalisms for the control of multi-physical energetic systems: COG and EMR", Systemic Design Methodologies for Electrical Energy Systems, Chap. 3, Wiley-ISTE, ISBN 9781848213883, October 2012.

[20] A.L. Allègre, A. Bouscayrol, and R. Trigui, "Flexible real-time control of a hybrid energy storage system for electric vehicles", IET Electrical Systems in Transportation, vol. 3, no. 3, pp. 79-85, March 2013.

[21] J. Solano Martinez, D. Hissel, M.C. Pera, and M. Amiet, "Practical control structure and energy management of a testbed hybrid electric vehicle", IEEE trans. on Vehicular Technology, vol. 60, no. 9,pp. 4139-4152, September 2011.

[22] P. Sandulescu, L. Idkhajine, S. Cense, F. Colas, X. Kestelyn, E. Semail, A. Bruyere, "FPGA implementation of a general space vector approach on a 6-leg voltage source inverter", IECON 2011 - 37th Annual Conference of the IEEE Industrial Electronics Society, Melbourne, Australia, November 2011, pp. 3482 - 3487

[23] W. Lhomme, P. Delarue, X. Kestelyn, P. Sandulescu, A. Bruyère, "Control of a combined multiphase electric drive and battery charger for electric vehicle", EPE'13 ECCE Europe Conference, Lille, France, September 2013

[24] W. Zhao, M. Cheng, K. T. Chau, R. Cao, and J. Ji, "Remedial Injected-Harmonic-Current Operation of Redundant Flux-Switching Permanent-Magnet Motor Drives," IEEE Transactions on Industrial Electronics, vol. 60, no. 1, pp. 151-159, 2013.

[25] G. Scarcella, G. Scelba, M. Pulvirenti, and R. D. Lorenz, "Fault-Tolerant Capability of Deadbeat-Direct Torque and Flux Control for Three-Phase PMSM Drives," IEEE Transactions on Industry Applications, vol. 53, no.7, pp. 5496-5508, 2017.

[26] S. Bolognani, M. Zordan, and M. Zigliotto, "Experimental fault-tolerant control of a PMSM drive," IEEE Transactions on Industrial Electronics, vol. 47, no.5, pp. 1134-1141, 2000.

[27] D. Flieller, N. K. Nguyen, P. Wira, G. Sturtzer, D. O. Abdeslam, and J. Merckle, "A self-learning solution for torque ripple reduction for nonsinusoidal permanent-magnet motor drives based on artificial neural networks", IEEE trans. on Industrial Electronics, vol. 61, pp. 655-666, 2014.

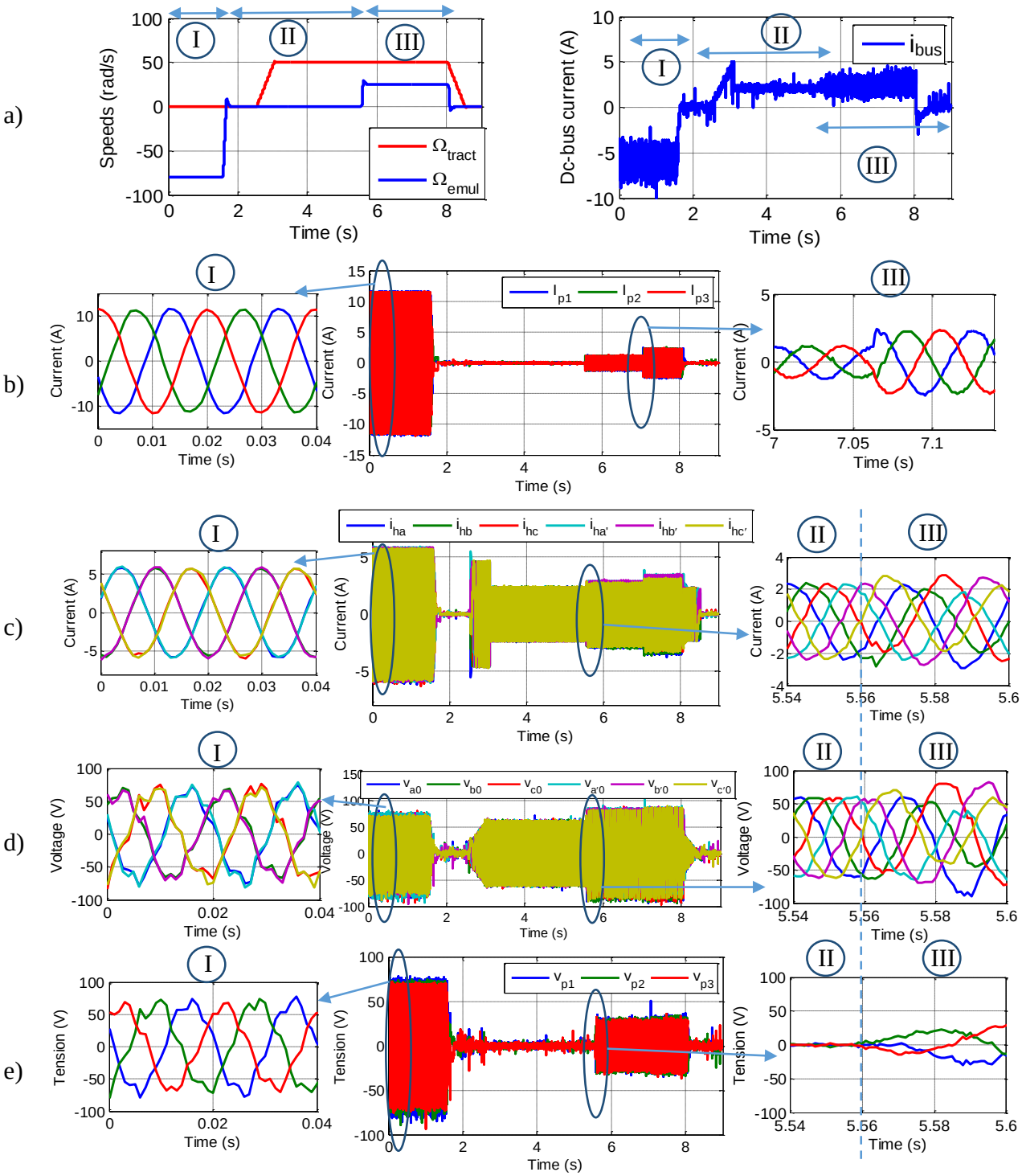

Fig. 6. Experimental results: a) Measured speeds of two machines (left) and the measured current of the DC bus (right); b) Grid currents; c) 6 currents of the 3-phase open-end winding machine; d) 6 references of voltage for the 3-phase open-end machine; e) Grid voltages (emulated by the back-EMF of a 3-phase PMSM).

Walter Lhomme (M'16) received the M.S. degree in 2004, and the Ph.D. degree in 2007, both in electrical engineering, from the University Lille 1, Sciences and Technologies, Villeneuve d'Ascq, France, specializing on graphical description tools and methods for modeling and control of electrical systems.

He worked as hybrid electric vehicle engineer within the Department Controls, Hybrid Vehicle Technologies Team at AVL Powertrain UK Ltd., England, for 1 year. Since September 2008 he has been engaged as Associate Professor at the Laboratory of Electrical Engineering and Power Electronics of Lille (L2EP), University of Lille, Faculty of Science and Technologies. Since 2008, he is the responsible of the experimental platform "electricity & Vehicle" of the L2EP at the University of Lille. His research activities deal with the graphical descriptions, modelling, control, energy management and hardware-in-the-loop simulations applied in hybrid and electric vehicles field.

Philippe Delarue received a Ph.D. degree from the University Lille1, Villeneuve d'Ascq, France, in 1989. Since 1991, he has been an Assistant Professor with Polytech'Lille, Villeneuve d'Ascq.

He is currently with the L2EP of Lille, University Lille1. His main research interests include power electronics and multi-machine systems.

Tiago José Dos Santos Moraes received the B.Sc. degree in Electrical Engineering from Institut National de Sciences Appliquées (INSA Lyon), Lyon, France, in 2011 and from the Universidade Federal do Rio de Janeiro (UFRJ), Rio de Janeiro, Brazil, in 2012 and the M.Sc. degree in Electrical Vehicles from the Arts et Métiers ParisTech, Lille, France, in 2013. In 2017, he received his PhD degree from Arts et Métiers ParisTech. His researches include fault-tolerant series-connected multiphase machines for aeronautics and aerospace industries.

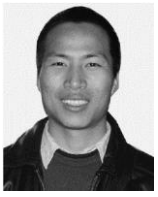

Ngac Ky Nguyen (M'13) received the B.Sc. degree in Electrical Engineering from Ho Chi Minh City University of Technology, Vietnam, in 2005, and the Ph.D. degree in Electrical and Electronic engineering from the University of Haute Alsace, France, in 2010. Since September 2012, he has been an Associate Professor with the Laboratory of Electrical Engineering and Power Electronics of Lille, Arts et Métiers ParisTech, Lille, France. His research interests include Modeling and Control of Synchronous Motors, Power Converters, and Fault-Tolerant Multiphase Drives. He has authored and co-authored 38 scientific papers and 5 book chapters.

Éric Semail (M'02) graduated from the Ecole Normale Superieure, Paris, France, in 1986, and received the Ph.D. degree with a thesis entitled 'Tools and studying method of polyphase electrical systems — Generalization of the space vector theory' from the University of Lille, France, in 2000. He became an Associate Professor at the Engineering School of Arts et Metiers ParisTech, Lille, France, in 2001 and a Full Professor in 2010. In the Laboratory of Electrical Engineering of Lille (L2EP), France, his fields of interest include design, modeling, and control of multiphase electrical drives (converters and ac drives). More generally, he studies, as a Member of the Control team of L2EP, multimachine and multiconverter systems. Fault tolerance for electromechanical conversion at variable speeds is one of the applications of the research with industrial partners in fields such as automotive, marine, and aerospace. Since 2000, he has collaborated on the publication of 27 scientific journals, 64 International Congresses, 5 patents, and 2 chapters in books.

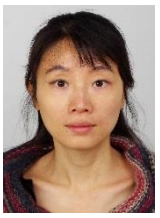

Keyu Chen, received her B.S. degree from Sichuan University (Chengdu, China) in 2000, her M.Sc. degree in 2006 and PhD degree in 2010 from University of Lille1 (France) all in electrical engineering. She worked for State Grid Corporation of China in China from 2000 to 2003. She participated one of cooperation research projects between L2EP (University of Lille1), FEMTO-ST (University of Franche-Comté) and IFSTTAR (Lyon Bron) from 2006-2010. In 2011, the project NEHC 'solutions for electric-mobility' led by her, has been awarded 2011 national competition to encourage innovative technology businesses, organized by Ministry of Higher Education and Research and OSEO ('Emergence' category, France). Now she is working as software team leader at Valeo-Siemens eAutomotive.

Since 2017, **Bénédicte Silvestre** is head of innovation of Valeo Siemens e Automotive (motor and power electronics). She has previously led during 8 years the activity of power electronics for Hybrid and Electric Vehicles application, for Valeo powertrain business group based in Cergy France. She is recognized as Valeo Senior expert in power electronics and mechatronic design. Before that, she has been three years in charge of advanced R&D projects for Engine control units product and electric motor drive product lines, including manufacturing processes and assembly technologies. From 2001 to 2005, she led power steering product line engineering in Johnson Controls Automotive Electronic. She started her carrier in 1994 as hardware designer then team leader in Electric Vehicle components team in SAGEM company, and developed charger, DCDC converter and inverter for PSA and Renault.

She graduated from engineering high school (ESIGELEC, Rouen, France) specialized in power electronics and electrotechnics, and a DEA (troisième cycle diplome d'études avancées) in automatism, system controls and electric motor control laws.